Available online at www.sciencedirect.com
ScienceDirect
Solid State Ionics 177 (2006) 2617–2624
SOLID STATE IONICS
www.elsevier.com/locate/ssi

Diffusional mechanism of deintercalation in $LiFe_{1-y}Mn_yPO_4$ cathode material

J. Molenda [a,*], W. Ojczyk [a], K. Świerczek [a], W. Zając [a], F. Krok [b], J. Dygas [b], Ru-Shi Liu [c]

[a] Faculty of Materials Science and Ceramics, AGH University of Science and Technology al. Mickiewicza 30, 30-059 Krakow, Poland
[b] Faculty of Physics, Warsaw University of Technology pl. Politechniki 1, 00-661 Warsaw, Poland
[c] Department of Chemistry, National Taiwan University Roosevelt Road, Taipei 106, Taiwan, R.O.C.

Received 29 June 2005; received in revised form 22 March 2006; accepted 29 March 2006

Abstract

The paper presents the investigations on the structural, electrical and electrochemical properties of Mn substituted phospho-olivines $LiFe_{1-y}Mn_yPO_4$ and of W, Ti or Al doped $LiFePO_4$. The microscopic nature of the observed macroscopic, metallic-like conductivity of W, Ti, Al doped phospho-olivine samples is discussed. Some fundamental arguments against the bulk type conductivity are presented.

A single phase, diffusional mechanism of deintercalation was found to appear for Mn-substituted $LiFe_{1-y}Mn_yPO_4$ samples in the whole range of lithium concentration, in contrast to the pure $LiFePO_4$, $LiMnPO_4$ and W, Ti, Al doped phospho-olivines, where a two-phase mechanism of electrochemical lithium extraction/insertion is observed.

Keywords: Phospho-olivine; $LiFe_{1-y}Mn_yPO_4$; Lithium diffusion; Cathode materials for Li-ion batteries; Intercalation

1. Introduction

A novel group of olivine based cathode materials for Li-ion batteries has emerged recently. $LiFePO_4$ and isostructural materials are chemically and thermally stable, environmentally benign and exhibit a high gravimetric and volumetric energy density. However, the most serious drawback arises from the insulating properties (electrical conductivity of the order of 10^{-10} S/cm at RT) of these materials, since the effectively working cathode material requires good electronic carrier distribution in the whole volume. In order to achieve the high current density of the phospho-olivine cathode many efforts have been undertaken, most of them being concentrated on the significant improvement of macroscopic electrical conductivity, either by optimization of carbon additives and microstructure of the material [1–4] or, alternatively, by obtaining the electrically conductive phospho-olivine [5]. The controversial report by Chung et al. [5] on the metallic type conductivity of $LiFePO_4$, achieved by doping phospho-olivine with Zr, Nb or W attracted great interest and caused the intensification of studies on the influence of dopants on the electrical conductivity of this material [6–8].

Both the low concentration of electronic carriers in stoichiometric $LiFePO_4$ and structural restrictions (one dimensional lithium diffusion paths) are responsible for limiting the kinetics of lithium extraction. Two-phase mechanism of lithium extraction/insertion observed in working $Li/Li^+/LiFePO_4$ cell is described by the following equation:

$$LiFePO_4 - xLi^+ - xe^- \leftrightarrow (1-x)LiFePO_4 + xFePO_4. \quad (1)$$

The goal of our work was to improve electrical conductivity of phospho-olivine based materials, as well as to change the mechanism of electrode reaction from the two-phase type to the diffusional one:

$$LiFePO_4 - xLi^+ - xe^- \leftrightarrow Li_{1-x}FePO_4. \quad (2)$$

We attempted to significantly improve the electrical conductivity of phospho-olivine by employing two different methods:

1. selective doping of lithium sublattice in $LiFePO_4$ with W^{6+}, Ti^{4+} or Al^{3+} ions

* Corresponding author.
E-mail address: molenda@uci.agh.edu.pl (J. Molenda).

0167-2738/$ - see front matter © 2006 Elsevier B.V. All rights reserved.
doi:10.1016/j.ssi.2006.03.047

2. a substitution of iron with manganese and therefore formation of $LiFe_{1-y}Mn_yPO_4$.

In this work the results of the structural, electrical and electrochemical measurements of the doped phospho-olivines are presented, together with properties of these compounds after the electrochemical deintercalation, in order to establish the delithiation mechanism.

2. Experimental

The W, Ti or Al doped phospho-olivines with the assumed chemical composition ($Li_xW_{0.01}FePO_4$, x: 0.99–0.94, $Li_{0.99}Al_{0.01}FePO_4$ and $Li_{0.99}Ti_{0.01}FePO_4$) were prepared from Li_2CO_3 (POCh, pure p.a.), $FeC_2O_4{\cdot}2H_2O$ (Aldrich, pure), $NH_4H_2PO_4$ (POCh, pure p.a.), and H_2WO_4 (Aldrich, pure p.a.), $Ti(OC_3H_7)_4$ or aluminium acetylacetate (Aldrich, 99%). The reactants were weighed in stoichiometric proportions and mixed in a mortar with an addition of iso-propanol. Thermal treatment was performed in two stages in the high purity argon flow. The first stage — decomposition of the reactants at 350 °C was continued for 12 h. After the first stage the reactants were cooled down to room temperature and again mixed in the mortar. The second stage — proper synthesis at 800 °C was continued for the next 12 h.

Pure $LiFePO_4$ and $LiFe_{1-y}Mn_yPO_4$ phospho-olivines were synthesized by a high temperature reaction using Li_2CO_3 (POCh, pure p.a.), $MnCO_3$ (Aldrich, pure p.a.), $FeC_2O_4{\cdot}2H_2O$ (Aldrich, pure) and $NH_4H_2PO_4$ (POCh, pure p.a.). The reactants were thoroughly ground in the mortar with some acetone added, then dried and pressed into pellets. The initial heating and synthesis were performed under high purity argon, with the following sequence of time/temperature regimes: 1.5 h at 100 °C (to remove water from the system), 2 h at 260 °C (to decompose iron oxalate), 3 h at 350 °C (to remove gaseous products and to initiate the synthesis). The final heating was performed at 750 °C for 24 h. This complex procedure was developed in order to avoid Fe^{2+} oxidation and to minimize the formation of phosphides and $Fe_{1-y}Mn_yP_2O_7$ [9]. The colour of the samples varied from dark grey for the samples with a high iron content to light grey for the samples with 55 at.% of manganese.

In the electrochemical studies, composite cathodes were used, containing 85 wt.% of $LiFe_{1-y}Mn_yPO_4$, 7.5 wt.% of graphite and 7.5 wt.% of carbon, the last being the product of the decomposition of a phenol–formaldehyde resin. The additives, namely electronic conductors were necessary because of the very high resistivity (10^{10} Ω cm) of the phospho-olivine. The additives constituted a highly conductive matrix in which the much less conductive olivine grains were embedded. This microstructure allows attaining nearly maximum theoretical capacity of the olivine at the lower current density [1,3].

The samples were characterized by XRD (Phillips X'Pert Pro), SEM (JEOL JSM 5400) and EDS measurements. The X-ray spectra were analysed by Rietveld method [10,11] using the X'Pert Plus software. Iron oxidation state and its local surrounding were characterized by ^{57}Fe Mössbauer spectroscopy at 300 K, with the spectrometer operating in a constant acceleration mode in transmission geometry and with a ^{57}Co (Rh) source. Moreover, the oxidation states of Fe and Mn were characterized by X-ray absorption near edge structure (XANES) measurements. The XANES measurements were carried out at Wiggler beam line BL 17C of National Synchrotron Radiation Research Center (NSRRC) at Taiwan. The electron storage ring was operated at the energy of 1.5 GeV, with a beam current of 100–200 mA. A Si(111) double-crystal monochromator was employed for the energy selection with a resolution ($\Delta E/E$) around $2\cdot10^{-4}$. The XANES spectra at Fe and Mn K-edge were recorded at the room temperature in transmission mode using gas-filled ionization chambers to measure the intensities of the incident and transmitted X-ray spectra. The spectra were then normalized with respect to the edge jump.

The specimens for the impedance spectroscopy measurements were shaped into flat pellets, ground with abrasive papers up to 2400 grit no. The electrodes were the thin films of gold, deposited on flat surfaces of the pellets by means of plasma spraying. Thus prepared specimens were inserted between the two mounting plates inside a spring holder. The measurements were performed in the argon flow of N5 purity. The impedance spectra were recorded using a laboratory set-up, comprising Solartron 1260 analyser and Keithley 428 current amplifier operating in the frequency range 10^{-2}–10^{7} Hz, with the alternating voltage excitation (rms value of 30 mV). The specimens were thermostated in the electric furnace with a constant voltage supply. The measurements within the temperature range 300–660 K were repeated every time when the measuring algorithm detected some impedance drift during the 30 min time of data acquisition (spectrum consisting of 160 frequencies).

The electrochemical extraction of lithium was performed in the $Li/Li^+/Li_{1-x}Fe_{1-y}Mn_yPO_4$ cells, consisting of a lithium metal anode, Selectipur LP71 electrolyte (EC:DEC:DMC 1:1:1, 1M $LiPF_6$, Merck), and a composite cathode prepared as described above. The charging curves of the cells, SEM and the lithium diffusion coefficient were determined as a function of lithium concentration in the cathode material. Lithium diffusion was measured by GITT (Galvanostatic Intermittent Titration Technique) technique, as described by Weppner and Huggins [12], with the current impulse of 300 μA/cm^2 lasting 130 s.

3. Results and discussion

3.1. Towards enhanced electronic conductivity of W, Ti, Al doped phospho-olivines

In his work [5] Chung et al. showed a spectacular increase (by seven orders of magnitude) in the electrical conductivity of $LiFePO_4$ obtained by introducing Nb^{5+}, Zr^{4+} or Mg^{2+} ions into the lithium sublattice. The activation energies of the electrical conductivity were about 0.05 eV at around room temperature. However, few attempts of this substitution reported in literature yielded rather ambiguous results [13–17]. On the one hand, calculations of the electronic structure for stoichiometric $LiFePO_4$, based on DFT methods with LDA or GGA

approximations, surprisingly indicated metallic or semiconducting properties of the materials with a narrow energy gap ~0.3 eV, being at odds with observed low conductivity (10^{-10} S/cm) of the system [18–20]. On the other hand, significantly improved predictions of the band structure of $LiFePO_4$ can be obtained by taking into account the orbital dependency of the exchange and Coulomb interactions [21–23]. Theoretical DFT calculations performed for the materials doped with magnesium or chromium, indicated the peaked density of states at the Fermi level, which could explain the observed metallic type conductivity [8,14].

Fig. 1(a, b) presents the results of the electrical conductivity and thermoelectric power measurements of the phospho-olivine samples doped with W^{6+}, Ti^{4+} and Al^{3+}. The observed values of conductivity 10^{-3}–10^{-4} S/cm together with low values of activation energies of the order of 0.02–0.1 eV could be interpreted as the appearance of metallization at the border of carrier localization. Low absolute values of thermoelectric power of the order of 10 μV/K and lack of the temperature dependence are characteristic features of the metallic state. This could be related with the formation of a narrow band created by the dopant. This kind of mechanism of semiconductor–metal transition upon doping is known in semiconductors as Mott's type transition [24]. For a critical N_c concentration, an overlapping of electronic wave functions of dopant occurs, leading to the formation of dopant conduction band. However, the systematic analysis of electrical properties of doped phospho-olivine samples gives rise to doubts whether the observed conductivity is the bulk one. The minor and rather random influence of the dopant type and its concentration on the conductivity, as well as the observed lack of critical dopant concentration, at which the dopant band could be formed are the basic objections. Moreover, the inhomogeneous dopant distribution observed sometimes (as seen by EDS microprobes) also leads to the same "metallic" behaviour of the material. The deintercalation proceeds via two-phase mechanism even for the high-conductive samples, as in the case of pure $LiFePO_4$.

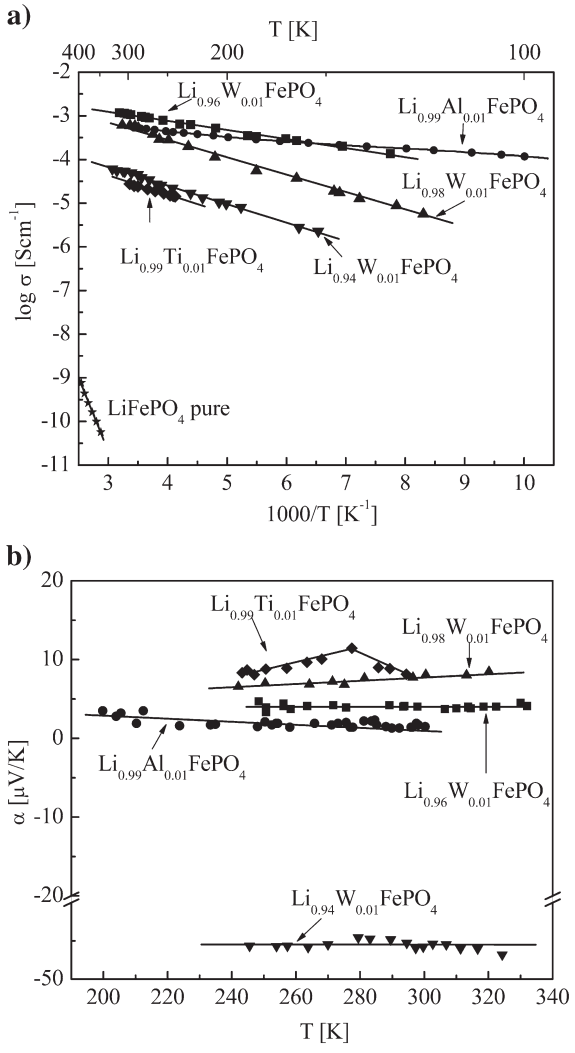

Fig. 1. a) Electrical conductivity of the phospho–olivine samples doped with W^{6+}, Ti^{4+} and Al^{3+}. b) Thermoelectric power of the phospho–olivine samples doped with W^{6+}, Ti^{4+} and Al^{3+}.

Recently performed calculations by Islam et al. [25] revealed, that doping the lithium sublattice with other ions (i.e. Al, Nb, Zr, Ti) is energetically unfavourable, hence highly improbable. Additionally, the results presented by Herle et al. [6], regarding phospho-olivine samples with lithium deficiency $Li_{1-x}FePO_4$, together with a stoichiometric $LiFePO_4$ obtained by a specific route and exhibiting the metallic conductivity are remarkable arguments against the idea of the bulk metallic conductivity of the phospho-olivine phase, attributed to the dopant atoms' presence. Given the fact that a stoichiometric sample would contain a slight lithium deficiency, leading to the presence of mixed valence state of iron, the existence of such Fe^{2+}/Fe^{3+} pair could not be responsible for the observed high electronic conductivity, since the iron–iron distance (4 Å) in the olivine structure is too large. Considering that in numerous M–O oxides, the metallic type conductivity appears for M–M distances smaller than 3 Å, it could be reasonable to bring into a question the actual cause for the observed increase in the electrical conductivity by seven orders of magnitude. Two possibilities should be taken into account: a conductive path created by the residual carbon, originating from the organic precursors used in synthesis and formation of iron phosphides or carbo-phosphides on the phosphate grains, forming thin, conductive path. Traces of the iron phosphides with content estimation around 4% of Fe_2P were observed by the surface sensitive CEMS technique (Fig. 2, [26]) or TEM [6]. As a consequence, we deal with a composite material with highly resistive grains and electronically conductive surfaces of the grains, the latter covered with iron phosphides, which create the conductive paths throughout the sample. The iron phosphides formation may be ascribed to the presence of internal reducing agents, Fe, $Fe_x(CO)_y$, C, CO and NH_3, being the products of the $FeC_2O_4 \cdot H_2O$, $NH_4H_2PO_4$ and Li_2CO_3 decomposition reaction during the synthesis. Therefore, the partial reduction of phosphate to iron phosphides cannot be neglected. For this reason, the actual influence of the dopant seems to be restricted only to the assumed lithium deficiency during the synthesis of the doped compound, which leads to the presence of the redox couple. As a result, the Fe^{2+}/Fe^{3+} redox couple acts as a catalyst

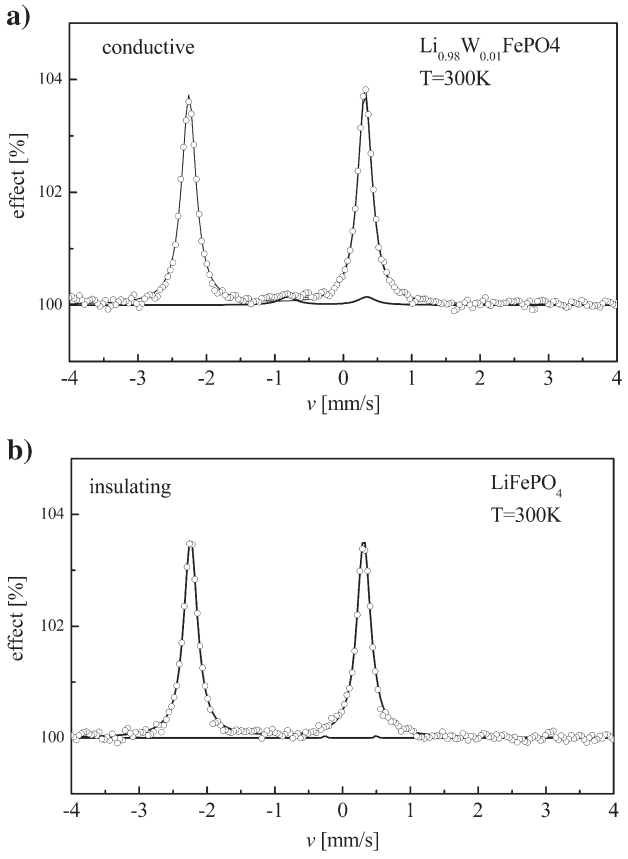

Fig. 2. CEMS (Conversion Electron Mössbauer Spectroscopy) for insulating and conductive phospho–olivine.

in the reduction of the $LiFePO_4$ into Fe_2P, the latter forming thin conductive layer over the sample's grains.

3.2. Towards enhanced electronic conductivity of substituted $LiFe_{1-y}Mn_yPO_4$ phospho-olivines

All of the synthesized $LiFe_{1-y}Mn_yPO_4$ samples were single-phase materials, with an orthorhombic olivine structure (P*nma*). The substitution of smaller Fe^{2+} ions [92 pm] by larger Mn^{2+} ions [97 pm] leads to the linear increase of all the cell parameters (Fig. 3), suggesting the existence of a solid solution in the whole substitution range ($0 \le y \le 1$). The oxidation states of manganese and iron were determined by means of XANES (Fig. 4a, b). Both elements appeared at +2 oxidation state for all the compositions. A detailed analysis of the determination of oxidation state for Fe in $LiFePO_4$ has been published by Prince et al. [27].

Yamada and coworkers demonstrated a phase diagram of $Li_{1-x}Fe_{1-y}Mn_yPO_4$ as a function of both lithium and manganese concentration, obtained by a chemical extraction of lithium from $LiFe_{1-y}Mn_yPO_4$ materials with compositions $0 \le y \le 1$ [28–30]. They stated that the best starting compositions of $LiFe_{1-y}Mn_yPO_4$ in terms of possible application in lithium batteries are those containing similar amounts of manganese and iron ions.

The temperature dependences of the electronic and ionic conductivity of $LiFePO_4$, $LiFe_{0.25}Mn_{0.75}PO_4$ and $LiFe_{0.45}Mn_{0.55}PO_4$ are shown in Fig. 5a and b. The electronic component of electrical conductivity of $LiFe_{0.45}Mn_{0.55}PO_4$ is by one order of magnitude higher as compared with the undoped $LiFePO_4$ (Fig. 5a). The activation energies of the

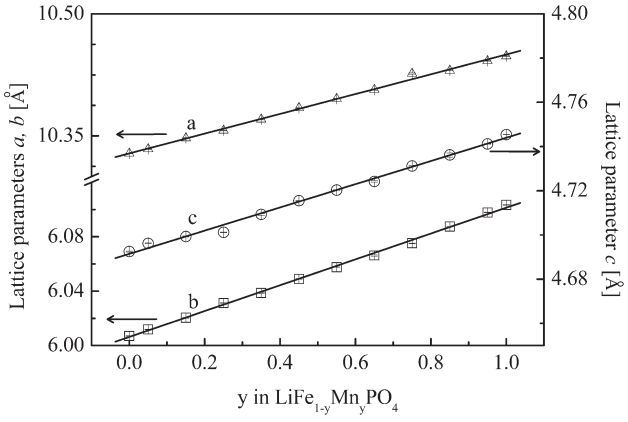

Fig. 3. Lattice parameters of $LiFe_{1-y}Mn_yPO_4$ as a function of manganese concentration.

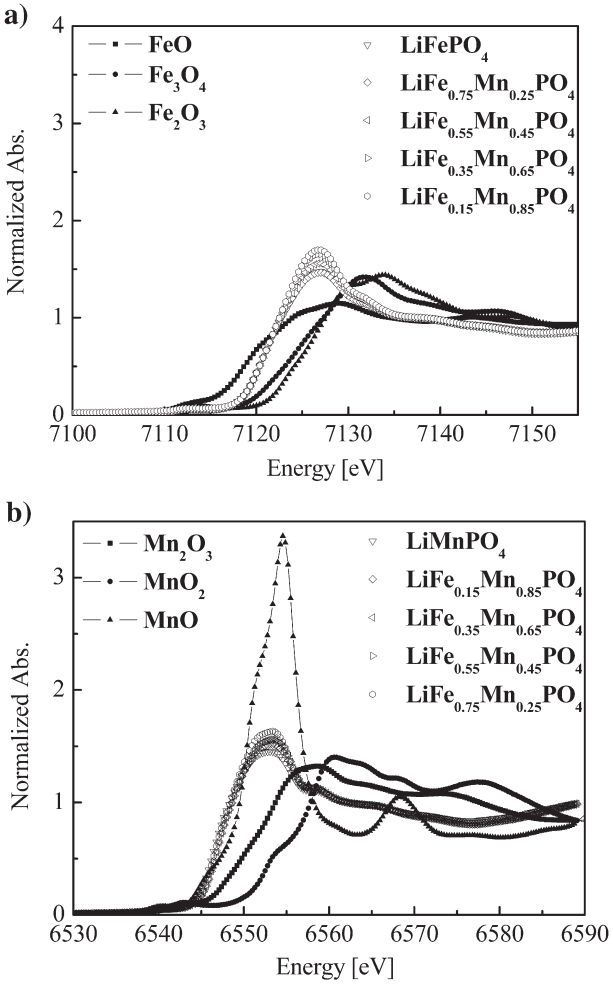

Fig. 4. a) XANES spectra on K–edge Fe for $LiFe_{1-y}Mn_yPO_4$. b) XANES spectra on K–edge Mn for $LiFe_{1-y}Mn_yPO_4$.

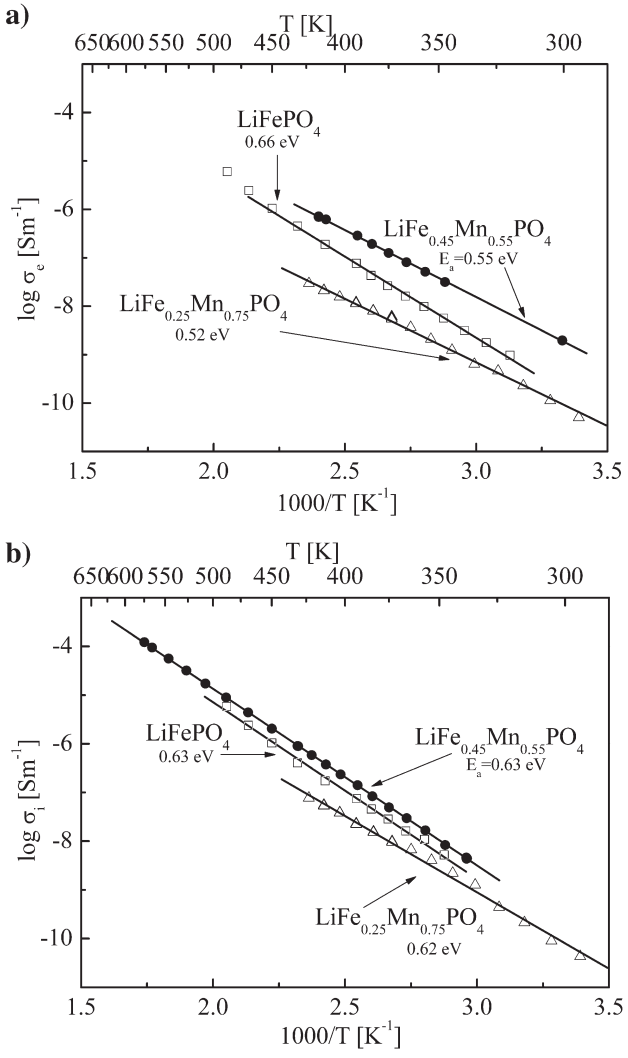

Fig. 5. a) Electronic conductivity of $LiFePO_4$, $LiFe_{0.45}Mn_{0.55}PO_4$ and $LiFe_{0.25}Mn_{0.75}PO_4$. b) Ionic conductivity of $LiFePO_4$, $LiFe_{0.45}Mn_{0.55}PO_4$ and $LiFe_{0.25}Mn_{0.75}PO_4$.

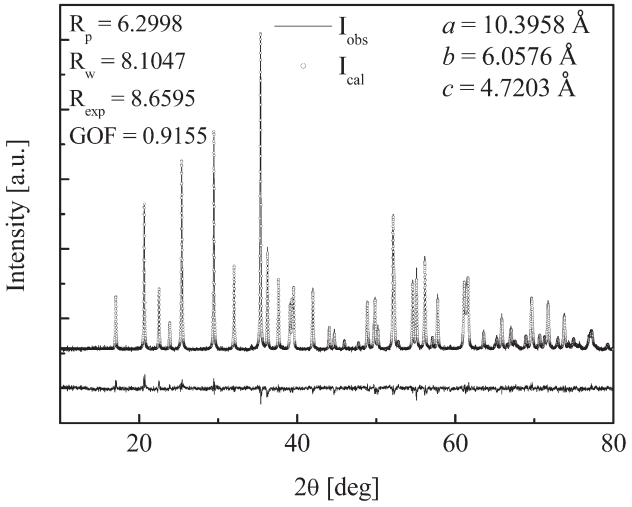

Fig. 6. X–ray spectrum of $LiFe_{0.45}Mn_{0.55}PO_4$.

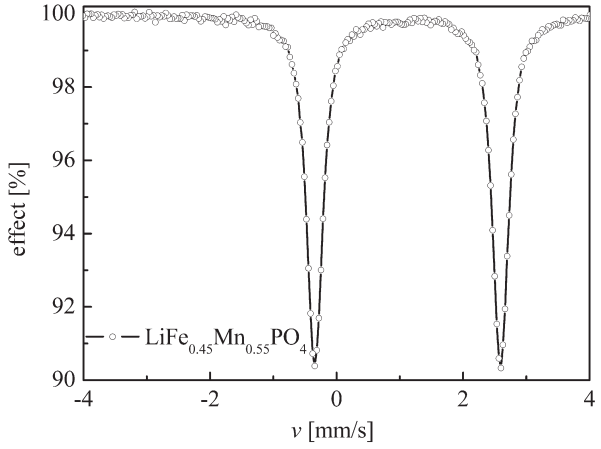

Fig. 7. Mössbauer spectrum of $LiFe_{0.45}Mn_{0.55}PO_4$.

electronic conductivity for $LiFe_{0.45}Mn_{0.55}PO_4$, $LiFe_{0.25}Mn_{0.75}PO_4$ and $LiFePO_4$ samples are 0.55, 0.52 and 0.66 eV, respectively. The lower activation energy of electronic conductivity for the iron–manganese phospho-olivine can be related to the presence of Fe^{2+}–Mn^{2+} pairs. The electronic configuration of manganese +2 is $3d^5$, while that of iron +2 is $3d^6$, which should facilitate the charge transport between these ions. However, for high spin configuration of Fe^{2+} and Mn^{2+} ions the expected improvement of electrical conductivity should not be significant. Structural relationships in phospho-olivine seems to favour the charge transport via Fe–O–Mn bonds, where the interionic distance between Mn^{2+} and Fe^{2+} is about 4 Å. The lower electronic conductivity of $LiFePO_4$ is related to the presence of only one type of transition metal ions, i.e. Fe^{2+} ($3d^6$). The room-temperature ionic conductivities of these compounds are similar (Fig. 5b). The activation energies of ionic conductivity, determined for pure and manganese-doped phospho-olivine are equal (0.63 eV) and close to the values calculated by numerical methods and to other experimental results [31,32]. It is worth noting that in spite of the slight electronic conductivity increase, the ionic conductivity of $LiFe_{0.45}Mn_{0.55}PO_4$ remains practically unchanged.

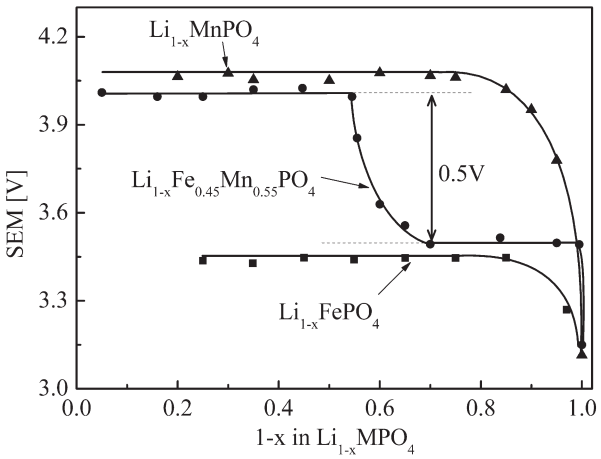

Fig. 8. SEM curves of the $Li/Li^+/Li_{1-x}MPO_4$ cells.

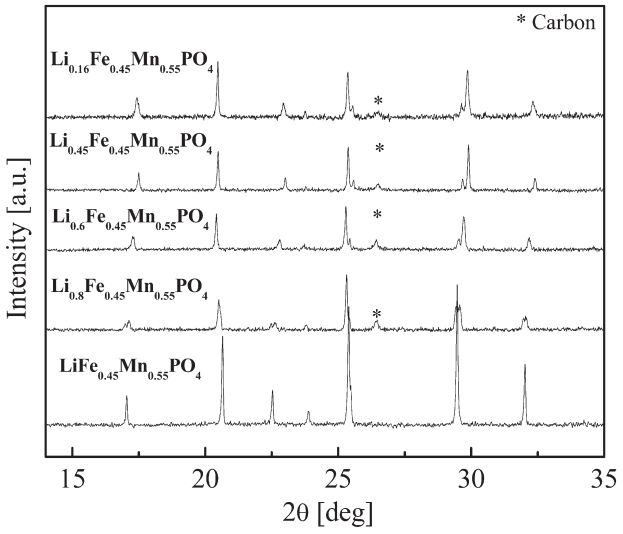

Fig. 9. X–ray patterns measured for samples obtained during electrochemical deintercalation in $Li/Li^+/Li_{1-x}Fe_{0.45}Mn_{0.55}PO_4$ cells.

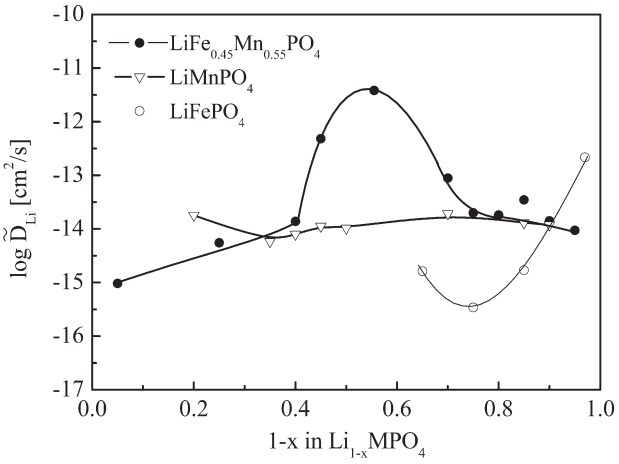

Fig. 11. Chemical diffusion coefficient of lithium concentration in $Li/Li^+/Li_{1-x}Fe_{0.45}Mn_{0.55}PO_4$ cells.

The $LiFe_{0.45}Mn_{0.55}PO_4$ composition, being the best conductive phospho-olivine, was chosen for structural, electrical and electrochemical studies. The obtained X-ray spectrum is shown in Fig. 6 and the results of Mössbauer spectroscopy studies are presented in Fig. 7. The quadrupole doublet indicates iron +2 in one crystallographic site. These results indicate that the synthesis route prevents the appearance of impurities containing Fe^{3+} [3].

Fig. 8 presents a SEM curve of the $Li/Li^+/Li_{1-x}Fe_{0.45}Mn_{0.55}PO_4$ cell with two characteristic potential plateaux. The first one, at a voltage of 3.5 V versus lithium electrode, is related to the iron oxidation $Fe^{2+} \rightarrow Fe^{3+}$, the second one at 4 V to manganese oxidation $Mn^{2+} \rightarrow Mn^{3+}$. The sudden steep change of voltage by about 0.5 V is observed at lithium content equal to 0.55. For comparison sake in Fig. 8 the analogous SEM curves were obtained for identical cells, but with $LiMnPO_4$ (the upper curve) and $LiFePO_4$ (the lower) as the cathode material are presented.

Fig. 9 shows X-ray patterns measured for samples obtained during electrochemical deintercalation in $Li/Li^+/Li_{1-x}Fe_{0.45}Mn_{0.55}PO_4$ cells. The evolution of cell parameters and the unit cell volume for deintercalated $Li_{1-x}Fe_{0.45}Mn_{0.55}PO_4$ samples,

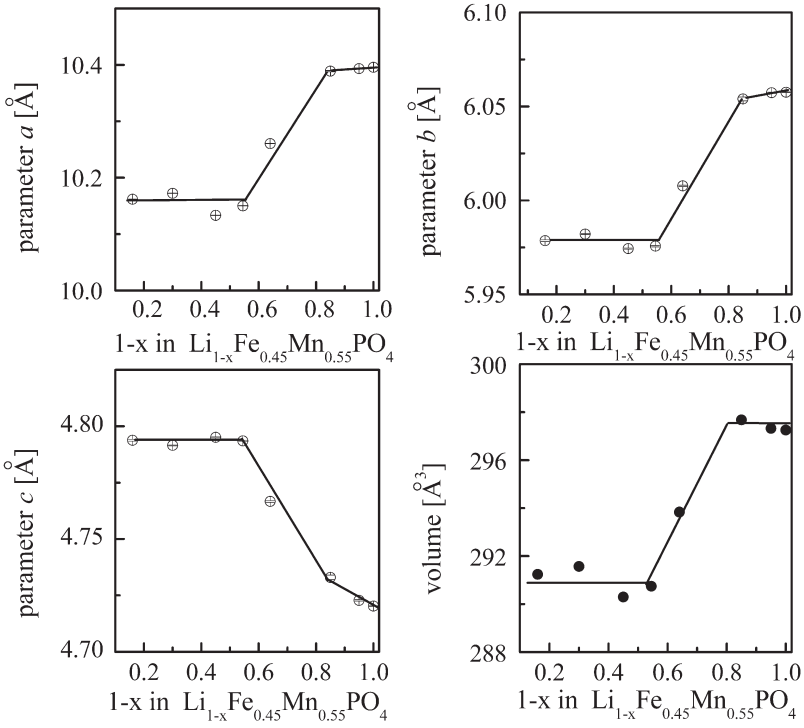

Fig. 10. Lattice parameters of $Li_{1-x}Fe_{0.45}Mn_{0.55}PO_4$ as a function of lithium concentration.

as a function of lithium content is presented in Fig. 10. In the composition range, where the voltage is 3.5 V and iron oxidation $Fe^{2+} \rightarrow Fe^{3+}$ takes place, a linear variation of a, b, c lattice parameters of the phospho-olivine with lithium content is observed up to $(1-x)_{Li}=0.55$ (Fig. 10). The diffusional mechanism of deintercalation process of $Li_{1-x}Fe_{0.45}Mn_{0.55}PO_4$ occurs within this lithium composition range. When lithium concentration decreases below 0.55, the X-ray spectra always indicate a single-phase material, but the lattice parameters remain constant (Figs. 9 and 10). It seems that this kind of behaviour can be explained on the basis of some earlier studies [33]. It has been stated, that during the lithium deintercalation at the voltage of 4 V, phospho-olivine phases with different lithium concentrations are formed. This observation seems to be in accordance with the model developed by Andersson [34], according to which delithiation of the phospho-olivines does not proceed by a radial mode but by a mosaic mode, involving the appearance of microregions with and without lithium in the cathode material. Yamada [28–30] has shown that the lithium deintercalation is a diffusional process at 3.5 V, while at 4 V, manganese oxidation $Mn^{2+} \rightarrow Mn^{3+}$ leads to the formation of the two phases. The different delithiation mechanism of phospho-olivine, observed by the authors at 4 V, may be related to the fact that in Yamada's experiments lithium was extracted chemically in a NO_2BF_4 solution. Such diverse behaviour for electrochemically and chemically deintercalated lithium manganese spinel leads to obtaining products with different physical and chemical properties, as it was demonstrated earlier [35].

In Fig. 11 we present the results of chemical diffusion coefficient of lithium measurements carried out during the deintercalation of $Li_{1-x}Fe_{0.45}Mn_{0.55}PO_4$, together with the data for pure $LiMnPO_4$ and $LiFePO_4$, where the electrode processes involve the two-phase mechanism in the whole range. A coexistence of $Fe^{2+}(3d^6)/Fe^{3+}(3d^5)$ and $Mn^{2+}(3d^5)$ in $LiFe_{1-y}Mn_yPO_4$ most likely enables local charge transport in the region $0.4<x_{Li}<0.7$ and therefore changes the electrode reaction from the two-phase mechanism to the diffusional one. As a consequence, the increase of chemical diffusion coefficient of lithium by the factor of 10^3 is observed. A discussion on the importance and applicability of the GITT technique for determining the diffusion coefficient of lithium in the series of olivine structured compounds can be found elsewhere [36].

Mössbauer effect measurements yield the evidence for the oxidation processes taking place in the course of lithium extraction. For the starting composition $Li_1Fe_{0.45}Mn_{0.55}FePO_4$ (Fig. 12a), the observed absorption pattern was satisfactorily fitted with only one quadruple doublet, originating from the single valence state of iron (Fe^{2+}), occupying a unique crystallographic site. For the subsequent, electrochemically deintercalated samples $Li_{1-x}Fe_{0.45}Mn_{0.55}FePO_4$ (Fig. 12b, c), the obtained spectra were unambiguously fitted with two doublets of different isomer shifts (IS) and quadruple splitting (QS), indicating the presence of Fe^{2+} and Fe^{3+} ions with relative ratio r varying with and matching the lithium content ($r=0.45-x/0.45$; $0.55 \le 1-x \le 1$). Nevertheless, the spectrum of the

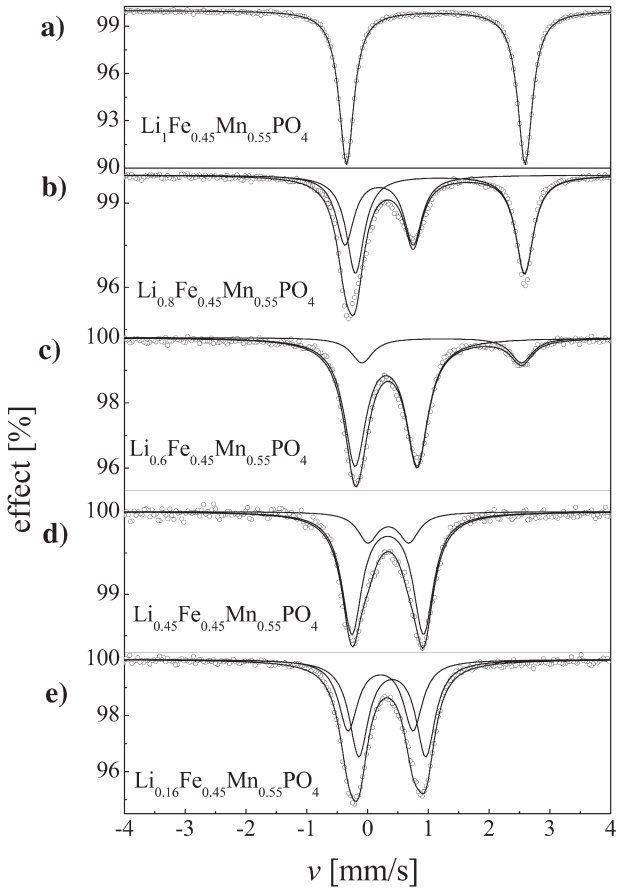

Fig. 12. Mössbauer effect measurements of the $Li_{1-x}Fe_{0.45}Mn_{0.55}PO_4$ cathode materials of the different lithium concentration.

$Li_{0.45}Fe_{0.45}Mn_{0.55}FePO_4$ sample also consists of two doublet components, despite the fact, that during this stage only Fe^{3+} is present in the sample. Further deintercalation (Fig. 12d) is related to the successive oxidation of Mn^{2+} and, as a consequence, changes local symmetry of the iron site, which was confirmed by the observed increase of the quadruple split for the doublets in the Mössbauer absorption pattern. It is also worth mentioning that the spectra given in Fig. 12(d, e) differ considerably from those presented in [28], where a conclusion of the appearance of a second phase was drawn. The two components are necessary to fit the spectra, but the observed significant widths of the absorption lines for these two components indicate rather continuous distribution of the QS parameter. From the above observations it follows that within the whole range of lithium concentration the process of its electrochemical extraction from the $Li_{1-x}Fe_{0.45}Mn_{0.55}FePO_4$ compound occurs via deintercalation mechanism. In other words, the material is a single-phase one, but rather inhomogeneous in the $0<(1-x)_{Li}<0.55$ deintercalation region.

4. Conclusions

The results obtained for the conductive W, Ti or Al-doped phospho-olivines have provided the strong arguments against the picture of bulk metallic conductivity, resulting from the presence of dopant atoms. It was shown that the partial

reduction of phosphates to iron phosphides during the synthesis is responsible for creation of phosphide conductive paths on the surface of the phosphate grains.

Coexistence of Fe^{2+} ($3d^6$) and Mn^{2+} ($3d^5$) in $LiFe_{1-y}Mn_yPO_4$ most likely enables the local charge transport, therefore changes the electrode deintercalation mechanism from the two-phase one to the diffusional one.

Acknowledgement

The work is supported by Polish Committee Scientific for Research under grant 4 T08A 020 25. The authors would like to thank Dr. M. Dudek for providing $Li_xW_{0.01}FePO_4$ samples.

References

[1] H. Huang, S.-C. Yin, L.F. Nazar, Electrochem. Solid-State Lett. 4 (2001) A170.
[2] Z. Chen, J.R. Dahn, J. Electrochem. Soc. 149 (2002) A1184.
[3] A. Yamada, M. Hosoya, S.-Ch. Chung, Y. Kudo, K. Hinokuma, K.-Y. Liu, Y. Nishi, J. Power Sources 119–121 (2003) 232.
[4] S. Franger, F. Le Cars, C. Bourbon, H. Rouault, J. Power Sources 119–121 (2003) 252.
[5] S.-Y. Chung, J.T. Bloking, Y.-M. Chiang, Nat. Mater. 1 (2002) 123.
[6] P.S. Herle, B. Ellis, N. Coombs, L.F. Nazar, Nat. Mater. 3 (2004) 147.
[7] S.-Y. Chung, Y.-M. Chiang, Electrochem. Solid-State Lett. 6 (2003) A278.
[8] C. Lampe-Onnerud, S. Dalton, P. Onnerud, D. Novikov, J. Shi, J. Treger, R. Chamberlain, 203rd Meeting of the Electrochemical Society, April 27–May 2, 2003.
[9] A. Yamada, S.-Ch. Chung, K. Hinokuma, J. Electrochem. Soc. 148 (2001) A224.
[10] H.M. Rietveld, Acta Crystallogr. 22 (1967) 151.
[11] H.M. Rietveld, J. Appl. Crystallogr. 2 (1969) 65.
[12] W. Weppner, R.A. Huggins, J. Electrochem. Soc. 124 (1977) 1569.
[13] J. Barker, M.Y. Saidi, J.L. Swoyer, Electrochem. Solid-State Lett. 6 (2003) A53.
[14] S. Shi, L. Liu, Ch. Ouyang, D.-S. Wang, Z. Wang, L. Chen, X. Huang, Phys. Rev., B 68 (2003) 195108.
[15] G.X. Wang, S. Bewlay, J. Yao, J.H. Ahn, S.X. Duo, H.K. Liu, Electrochem. Solid-State Lett. 7 (2004) A503.
[16] D.X. Gouveia, V. Lemos, J.A.C. de Paiva, A.G. Souza Filho, J. Mendes Filho, Phys. Rev., B 72 (2005) 024105.
[17] G.X. Wang, S. Bewlay, S.A. Needham, H.K. Liu, R.-S. Liu, V.A. Drozd, J.-F. Lee, J.M. Chen, J. Electrochem. Soc. 153 (2006) A25.
[18] Y.-N. Xu, S.-Y. Chung, J.T. Bloking, Y.-M. Chiang, W.Y. Ching, Electrochem. Solid-State Lett. 7 (2004) A131.
[19] J.M. Osorio - Guillen, B. Holm, R. Ahuja, B. Johansson, Solid State Ionics 167 (2004) 221.
[20] Y.-N. Xu, W.Y. Ching, Y.-M. Chiang, J. Appl. Phys. 95 (2004) 6583.
[21] F. Zhou, C.A. Marianetti, M. Cococcioni, D. Morgan, G. Ceder, Phys. Rev., B 69 (2004) 201101.
[22] F. Zhou, K. Kang, T. Maxisch, G. Ceder, D. Morgan, Solid State Commun. 132 (2004) 181.
[23] F. Zhou, C. Cococcioni, C.A. Marianetti, D. Morgan, G. Ceder, Phys. Rev., B 70 (2004) 235121.
[24] N.F. Mott, E.A. Davis, Electronic Processes in Noncrystalline Materials, Clarendon Press, Oxford, 1971.
[25] M.S. Islam, D.J. Driscoll, C.A.J. Fisher, P.R. Slater, Chem. Mater. 17 (2005) 5085.
[26] J. Marzec, W. Ojczyk, J. Molenda, Mater. Sci. (Poland) 24 (2006) 69.
[27] A.A.M. Prince, S. Mylswamy, T.S. Chan, R.-S. Liu, B. Hannoyer, M. Jean, C.H. Shen, S.M. Haung, J.F. Lee, G.X. Wang, Solid State Commun. 132 (2004) 455.
[28] A. Yamada, Y. Kudo, K.-Y. Liu, J. Electrochem. Soc. 148 (2001) A747.
[29] A. Yamada, Y. Kudo, S.-Ch. Chung, J. Electrochem. Soc. 148 (2001) A960.
[30] A. Yamada, Y. Kudo, K.-Y. Liu, J. Electrochem. Soc. 148 (2001) A1153.
[31] K. Rissouli, K. Benkhouja, J.R. Ramos-Barrado, C. Julien, Mater. Sci. Eng., B 98 (2003) 185.
[32] D. Morgan, A. Van der Ven, G. Ceder, Electrochem. Solid-State Lett. 7 (2004) A30.
[33] W. Ojczyk, J. Marzec, K. Świerczek, J. Molenda, Defect Diffus. Forum 237–240 (2005) 1299.
[34] A.S. Andersson, J.O. Thomas, J. Power Sources 97–98 (2001) 498.
[35] J. Molenda, W. Ojczyk, M. Marzec, J. Marzec, J. Przewoźnik, R. Dziembaj, M. Molenda, Solid State Ionics 157 (2003) 73.
[36] P.P. Prosini, M. Lisi, M. Zane, M. Pasquali, Solid State Ionics 148 (1–2) (2002) 45.